

## NUMERICAL MODELING OF A VERY LARGE CRUDE OIL CARRIER USING ANSYS CFX: A CASE STUDY OF SALINA

(DOI No: 10.3940/rina.ijme.2019.a4.560)

**H Hakimzadeh**, Department of Marine Sciences, Faculty of Natural Resources and Environment, Science and Research Branch, Islamic Azad University, Iran, **M Torabi Azad\***, Department of Physical Oceanography, North Tehran Branch, Islamic Azad University, Iran, **M A Badri**, Isfahan University of Technology, Research Institute for Subsea Sciences & Technology, Iran and **F Azarsina**, Department of Marine Structures, Faculty of Engineering, Science and Research Branch, Islamic Azad University, Iran and **M Ezam**, Department of Marine Sciences, Faculty of Natural Resources and Environment, Science and Research Branch, Islamic Azad University, Iran

### SUMMARY

Specification of the frictional resistance values of tankers is the first step in managing their fuel consumption. Drag force of a very large crude oil carrier has been calculated using the numerical simulation method. With application of the ANSYS CFX software, the scaled model of the mentioned tanker with the length of 2.74 meters, width of 0.5 meters, draft of 0.17 meters was used for numerical simulation of the drag force in the tanker. Furthermore, the numerical solution of the drag force of the model was performed for 5 different speeds ranging from 0.65 to 0.85m/s. Based on the validations carried out, with mean drafts of 8 and 16.5cm, the difference between the results of the experimental and numerical models at low speeds was about 7%. However, the difference was observed to be up to 15% at higher Froude numbers. The results of the present study with respect to the SALINA are based on the method presented in ISO 19030 standard addressing the performance monitoring during vessel servicing.

### 1. INTRODUCTION

Shipping companies are constantly involved in the development and improvement of their fleet operations as well as application of optimum fuel consumption techniques. Hence, a good number of researchers are concerned about the identification and minimization of the factors affecting the resistance on the vessels' hull taking advantage of various scientific methods. In comparison with vessels traveling shorter distances, vessels traveling long voyages have fewer options for reducing or optimizing their fuel consumption. That is why it is very crucial to recognize the effect of the hull and propeller roughness on the skin friction and fuel consumption of an ocean-going tanker in various marine environmental conditions. Increasing drag forces leads to an increase in fuel consumption. The most expensive operating cost of a vessel during a voyage is related to the cost of its fuel consumption, which accounts for more than half of the total cost of a voyage. In this regard, the 19030 standard, aimed at monitoring the optimal performance of the vessel, has provided guidelines and scientific methods that are constantly being developed and updated. According to the mentioned standard, the use of computational fluid dynamics to estimate the resistance of a vessel to various drafts is of great significance (Park, et al, 2017). Numerical methods performed using computational fluid dynamics software impose less cost on the owners and provide more details of the simulation results. However, due to lesser accuracy of the results, the findings of the numerical model should be compared with those of the experimental simulation to pursue the validation goals. One of the problems encountered in identifying the drag of vessels' hull is scaling the small-scale roughness of their hull, in proportion to their full-scale dimensions. In recent years, direct numerical simulation (DNS) has been

used as a more reliable scientific method to thoroughly comprehend the physics of the flow on the vessels' sides. However, it must be mentioned that this method can only be implemented on a limited scale of Reynolds numbers. In 2004, Zalek, et al, has conducted a research addressing the effects of drag. Van et al. (1998) measured the flow around a very large crude carrier. Ogiwara et al. (1994) conducted studies on series 60 ships and calculated the pressure distribution around the hull surface. Jones and Clarke (2010) performed the numerical simulations of the current flow around a warship with the application of the ANSYS Fluent software. Obreja et al. (2005) have conducted several experimental tests on a bulk carrier. Korkut and Usta (2013) performed studies on five different types of aluminum plate, which examined increasing the resistance of the ship's hull in response to increasing the hull roughness with the application of a computational fluid dynamics model. Furthermore, Lungu (2007) conducted a research on a three-dimensional flow of surface turbulence around a liquid petroleum gas carrier. In 2009, Donnelly focused on the effect of turbulent boundary layer on the ship resistance. Moreover, Jakobsen (2010) presented the turbulent model of transverse flows entered on the vessel body. Hakan et al. (2007) calculated the resistance of a vessel model and compared the obtained value with the experimental results. Banks et al. (2010) quantified the resistance components of a container ship using ANSYS CFX software and compared the results with the experimental findings.

The purpose of the present study is to measure the hull drag force of SALINA. The findings will pave the way for future studies to use the calculated drag force values to measure the actual increase of vessels' fuel consumption and involuntary reduction of their speed with consideration of the standard 19030 guidelines

during servicing. It is worth mentioning that the increased fuel consumption and reduced speed are due to increased frictional resistance, which is the result of changes in the hull and propeller roughness and the physical conditions of the marine environment. In the presented study, two methods are applied to evaluate drag force of SALINA in both laden and ballast conditions. Details of the specifications are presented in Table 1 and Figure 1. In order to validate the obtained findings, the results of numerical simulation and experimental model have been compared. The results of the present study are generalizable to not only the SALINA but also to three similar oil tankers in the fleet of National Iranian Tanker Company.

Furthermore, after the disaster of the MT. Sanchi (one of the four tankers similar to the SALINA) in the China Sea, the results of this study could be a prelude to the initiation of scientific research on numerical simulation of the physical effect of the sea environment on maneuverability, engine, body movements, and interaction of the cargo and tanks of the MT. Sanchi before and after the collision, resulted in its explosion and sinking.

Table 1. Specifications of SALINA

Year of built	2009
Length Overall	274.18 m
Breadth (Extreme)	50 m
Designed draft	17.023 m
Summer deadweight displacement in summer draft	164040 MT.
displacement in summer draft	189187 MT.
Engine power (M.C.R.)	18660 KW.
Service speed	15.40 Knots



Figure 1. SALINA (EX. MT. Sarv)

## 2. PRINCIPLES AND METHODS

The experimental model of this tanker at a scale of 1:100 and in accordance with the International Towing Tank Conference guidelines was constructed. The specifications of the model are presented in Table 2 and Figure 2.

In this study, an unstructured integrated grid was generated in the entire solution field using the CFX software. Required corrections on the vessel geometry were performed and its quality was confirmed

(Figure. 3). The next steps included generating solution fields, creating a computational grid and improving its quality, entering the prepared computational grid to the pre-processing section for modeling, and eventually extracting results in the post-processing section.

Table 2. Dimensions of experimental model of SALINA

Length (mm)	Width (mm)	Height (mm)	Draft (mm)
2741	500	230	170



Figure 2. Painted and scaled model of the SALINA

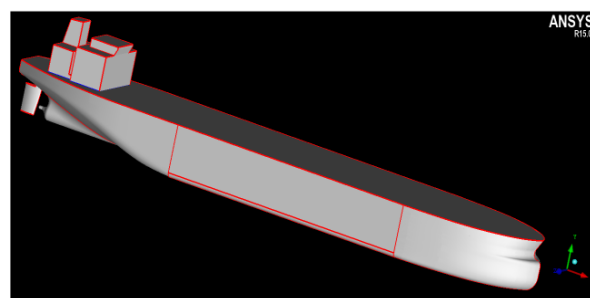


Figure 3. Corrected geometry of SALINA

### 2.1 GOVERNING EQUATIONS

The equations governing the fluid flow field are the same as Navier-Stokes equations. It is very challenging to directly solve the turbulent flows due to the effect of their disordered circular motions. In response to the mentioned difficulty, the averaged Navier-Stokes equations (RANS) were used, which are presented as equations 1 and 2 (White, 2015):

$$\frac{\partial \bar{u}_i}{\partial x_i} = 0 \quad (1)$$

$$\frac{\partial \bar{u}_i}{\partial t} + \frac{\partial \bar{u}_i \bar{u}_j}{\partial x_j} = -\frac{1}{\rho} \frac{\partial p}{\partial x_i} + \frac{\partial}{\partial x_j} \left\{ \nu \left( \frac{\partial \bar{u}_i}{\partial x_j} + \frac{\partial \bar{u}_j}{\partial x_i} \right) \right\} - \frac{\partial \bar{u}_i \bar{u}_j}{\partial x_j} + f_i \quad (2)$$

In these equations, the Reynolds stress ( $\bar{u}_i \bar{u}_j$ ) was added to the equations. In this study, the k-ε turbulence model was used to model Reynolds stress in the averaged equations of Navier Stokes. The turbulence model k-ε uses empirical functions to model the near-wall boundary layers. At the maximum true speed of the vessel (16.5

knots), corresponding speed of the model was 0.85 m/s and the dimensionless Reynolds number was equal to  $2.672 \times 10^6$ . To calculate the thickness of the first layer, the following experimental equation was used

$$\Delta y = 8.6Ly^+ Re^{-13/14} \quad (3)$$

where L is the length,  $y^+$  is the dimensionless height of the first layer (Figure. 4), and  $\Delta y$  is the thickness or dimension of the first layer within the boundary layers.

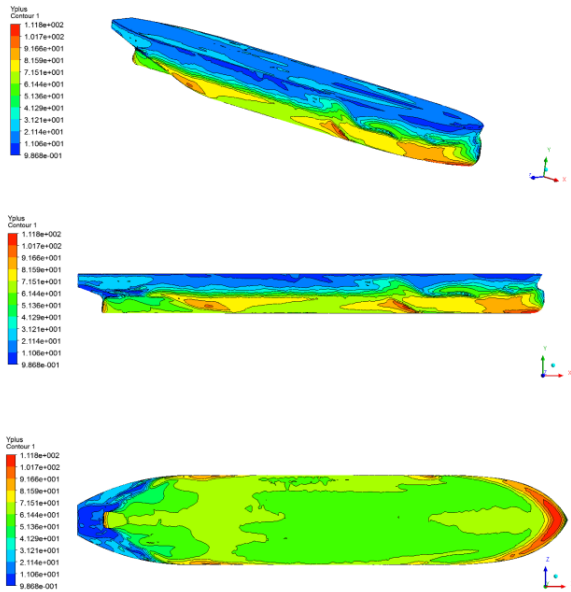


Figure 4. Distribution of  $y^+$  in three different faces on the vessel's hull in draft of 8cm and speed of 0.85m/s

## 2.2 GRID GENERATION

The computational grid required in this research was generated using the pattern of the Octree grid and implementation of the Delaunay grid model on it (combination of two grid generation approaches) (Figure. 5).

Then, by improving the quality and increasing the grid resolution, the boundary layer grid was produced on the smooth grid. Table 3 shows Specifications of the computational grid, including total number of knots & elements in both model drafts of 8 & 16.5cm.

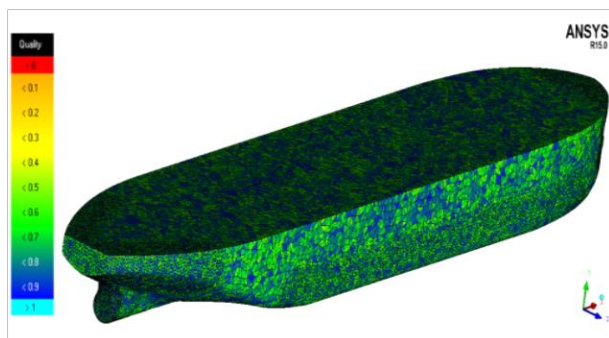


Figure 5. The elements produced on the vessel surface in terms of the quality of each element

Table 3. Specifications of the computational grid

Solution field status	Draft (cm)	Grid structure	Total number of elements	Total number of knots
Entire field	8	unstructured	4667046	933876
Entire field	16.5	unstructured	4657860	929653

Due to the necessity of an accurate examination of the free surface in each of the two drafts of 8 and 16.5 cm, the geometric complexities, and severe variations of the flow variables in some parts of the computational domain such as the bow and stern segments, the computational grid around the free surface (Figure. 6) was sufficiently accumulated (i.e. more meshes with the small sizes were applied) (Figures. 7 & 8).

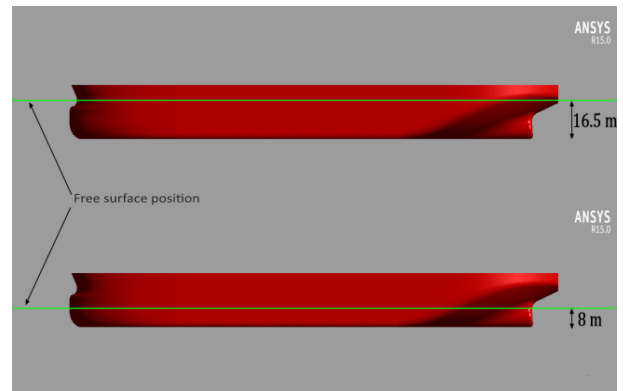


Figure 6. Status of free surface in drafts of 8 and 16.5 cm.

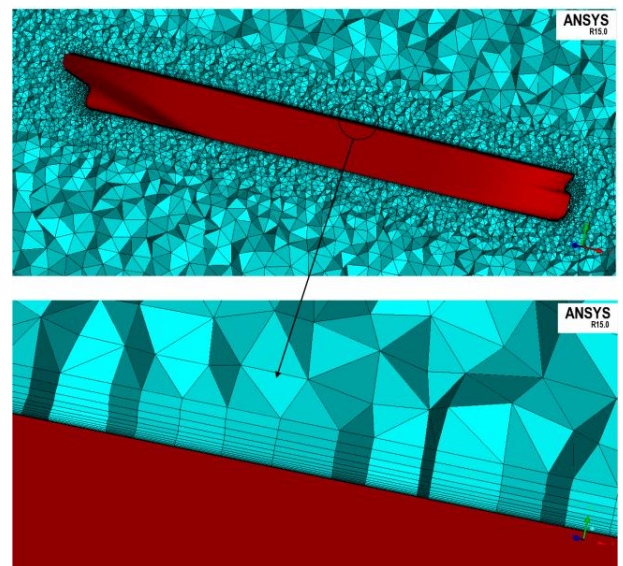


Figure 7. Representation of prismatic elements produced on the hull of vessel to perform the boundary layer analysis

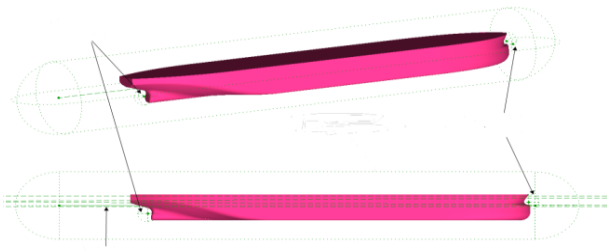


Figure 8. Accumulated areas of grid

### 2.3 GENERATION OF THE SOLUTION FIELD

In performing the analyses using computational fluid dynamics, the construction and quality of the computational grid generated for the model was of great value since it had great effects on the convergence, accuracy, and precision of the obtained results.

In the present analysis, one single solution field was used to construct an unstructured grid and to perform numerical analyses. The advantage of applying this approach was grid integrity and increased stability of the solution (Figures. 9 & 10).

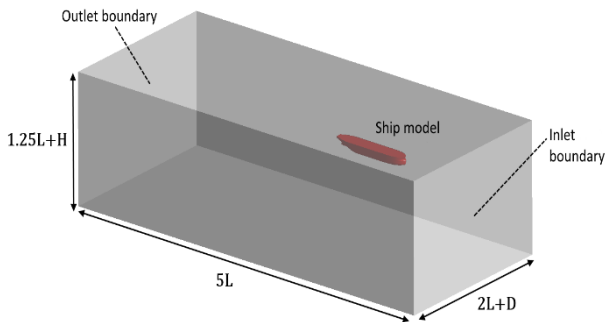


Figure 9. The domain and its dimensions

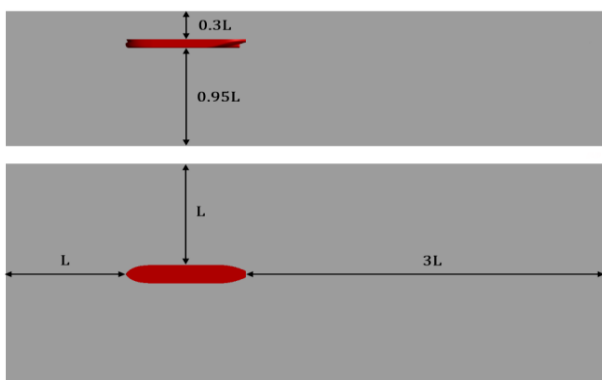


Figure 10. Status of the domain's boundary in relation to the ship's model

### 2.4 BOUNDARY CONDITIONS

First, the solution grid was called in the pre-processing section of the software. The boundary conditions were applied to the grid and the problem was about to be solved. For the entrance boundary, flow with the steady state was used as the boundary condition of the momentum equations. The boundary condition in the output of the grid was considered as the output flow type. In other words, distributions of the hydrostatic pressure in the water phase and the stable atmospheric pressure in the air phase were used as the boundary conditions for the output of the momentum equations.

Identical volume fraction profile was used in both the input and output boundaries. For turbulence equations, the development condition (zero gradient) was used. The free slip condition, whose shear stress was zero, was used for the side walls of the solution field and the upper and lower boundaries. In this case, the perpendicular velocity to the surface was zero and the tangential velocity was exactly equivalent to the calculated value in the first node after the wall. In the solver section of the software, the time step for free flow was selected based on the ratio of the length scale (length of the vessel) to the speed scale. The residual values were one of the most fundamental indicators in the convergence of repetitive numerical calculations, which directly determined the error rate in the solving equations. Over the time of performing all the equations, the convergence index in all numerical calculations was considered to be  $10^{-4}$ .

### 2.5 SIMULATION OF THE EXPERIMENTAL MODEL

The purpose of performing the model tests in the towing tank was to determine the drag force values of the SALINA and to compare the results with those of the numerical simulation. To meet the mentioned objective, the model of SALINA was designed and constructed at the scale of 1:100 and geometric accuracy of 0.05 mm with the length of 2.74 meters, width of 0.5 meters, draft of 0.17 meters, and height of 0.23 meters. The constructed model was in accordance with ITTC standards. To measure the drag force of the model, tests were performed in accordance with the numerical model in the towing tank at five different speed values ranging from 0.65 to 0.85 m/s (equivalent to the actual speeds of the vessel, i.e. 12.5, 13.5, 14.5, 15.5, and 16.5 knots). The process of conducting the hydrodynamic tests inside the towing tank involved determining test implementation scenario, preparing the model to perform the test, adjusting the force measurement system, installing the model into the towing carriage, performing the tests according to the predetermined scenario, extracting the data from the system, analyzing the data, and presenting the obtained results. The towing tank of subsea R & D center of Isfahan University of Technology (Figure. 11) was used to carry out the experimental simulation. The length, width, and depth of the mentioned tank were 108, 3, and 2/2 meters, respectively.



Figure 11. Towing tank of subsea R & D center of Isfahan University of Technology

According to Table 4, the towing tests of the model were carried out at drafts of 8 and 16.5 cm and at five different speeds. The values obtained for the drag force of the model were recorded digitally for each test. The process of unifying and eliminating incomplete information was performed for each test. The total resistance coefficient was calculated using the drag force of the model. By subtracting the frictional resistance coefficient and air resistance from the proposed method by ITTC, the wave resistance coefficient of the model, which was equal to the wave resistance coefficient of the ship, was calculated. By adding coefficients of frictional resistance and air resistance as well as correction values resulted from the difference between the roughness of the surface of the prototype and that of the vessel to the wave propagation coefficient of the ship, the total resistance coefficient of SALINA and the resulting drag force of the ship at desired speeds were obtained.

Table 4. Model tests in the towing tank

Number of whole tests	Number of repetitions	Number of tests	Model speed (m/s)	Model draft (cm)
10	2	5	0.65	8
			0.70	
			0.75	
			0.80	
			0.85	
10	2	5	0.65	16.5
			0.70	
			0.75	
			0.80	
			0.85	

### 3. RESULTS

#### 3.1 EXAMINATION OF THE INDEPENDENCE OF RESULTS OBTAINED FROM THE SOLUTION GRID

In order to verify the independence of the simulation results obtained from the computational grid, five grids with the specifications presented in Table 5 were considered.

Table 5. Specifications of the computational grids to evaluate the grid

Grid quality	Total elements	$y^+$
grid 1	1698528	60
grid 2	3026562	60
grid 3	4657860	60
grid 4	6982774	60
grid 5	9586322	60

To examine the independence of the numerical results obtained from the computational grid, the drag force of the tanker was extracted in the most critical simulation mode, that is to say draft of 0.165 meters and speed of 1.55knot (equivalent to 0.7974m/s), for each of the modes presented in Table 5. The results are presented in Figures 12 and 13.

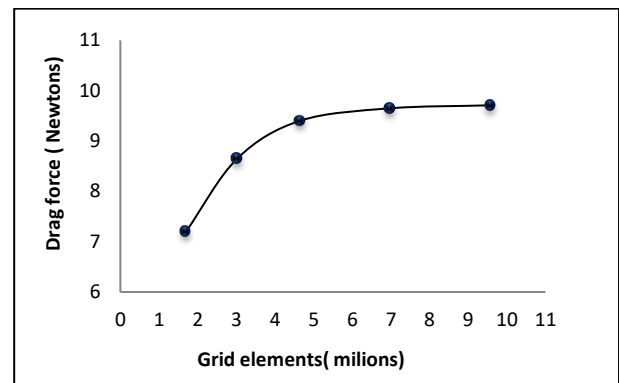


Figure 12. Drag force variations of the ship and the solution grid quality

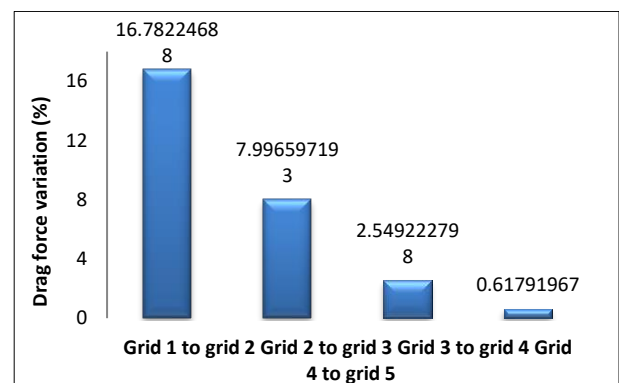


Figure 13. Drag force variation percentage of the ship in response to variations of grid type

As indicated in Figure. 15, by changing the grid from 1 to 2 and from 2 to 3, the drag force revealed changes of 16.8% and about 8%, respectively. Changing the grid from 3 to 4 and 4 to 5, the drag force of the ship presented the changes of 2.5% and 0.6%, respectively. Due to the high grid volume in the 5th mode and the 2.5% change of grid 3 compared to the very multi-mode grid 4, grid 3 was used as the optimal grid in the analyses.

### 3.2 RESULTS OBTAINED FROM THE DRAG FORCE VALUES

The drag force values of the SALINA at the desired speeds in both laden and ballast conditions (drafts of 8 and 16.5cm) were extracted from the post-processing section of the software. The values are indicated in Table 6 and Figure 14.

Table 6. Drag force values of the Saline tanker at desired speeds in both laden and ballast conditions

Draft (cm)	Ship's speed (m/s)				
	0.643	0.6945	0.7459	0.7974	0.8488
8	4.2928	4.876	5.53	6.17	6.89
	(N)	(N)	(N)	(N)	(N)
16.5	6.36	7.28	8.31	9.4	-
	(N)	(N)	(N)	(N)	-

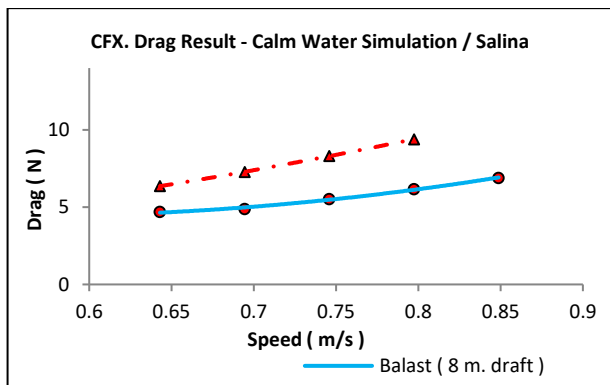


Figure 14. Drag force variation in response to speed and draft variations

Table 7. Differences between drag values calculated in the experimental and numerical models (CFX)

Draft of		Speed (m/s)				
		0.64	0.69	0.75	0.80	0.85
16.5cm.	Exp. model	6	6.76	7.79	8.87	10.79
	CFX	6.36	7.28	8.31	9.4	
Model & CFX deviation (%)		5.7	7.1	6.3	5.6	
8cm.	Exp. model	4.14	4.62	4.68	5.49	5.92
	CFX	4.29	4.87	5.53	6.17	6.89
Model & CFX deviation (%)		3.5	5.1	15.4	11	14.1

### 3.3 VALIDATION

Comparing the results of previous studies, predicting the numerical and laboratory values of a ship drag force revealed that the calculated drag of the ship's hull in the towing tank, including frictional resistance and wave resistance, provided a more realistic estimate (Noblesse, et al, 2013 & Huang, et al, 2013). The computational error of this method for a large part of ships with different weights has been considered to be within the acceptable range of 10% (Yang, et al, 2013). The results of a previous research on a bulk carrier indicated that the results of numerical simulation using the ANSYS FLUENT software and results of the experimental model at low and high speeds presented differences up to 5 and 13%, respectively. Moreover, the CFD-derived drag force value has always been greater than the values obtained from the experimental model of the bulk carrier (Ebrahimi, 2012). Table 7 compares the results of the numerical modeling and experimental simulation of SALINA, which are in line with the results of previous studies. In the case of 16.5cm draft, the difference between the drag force value of the numerical and experimental model in its maximum status is about 7%; however, this difference was observed to be 15% in the 8 cm draft. The reason for the observed error may be related to the weakness of the CFX software during simulation of the wave resistance of the model at higher speeds. There was less difference at lower speeds. In both drafts, the drag force value obtained from the numerical model was always higher than that of the experimental model (Figure. 15). Furthermore, the trend of results obtained from the experimental model tests and CFD simulation tests in the draft of 16.5cm were more consistent than the results obtained in the 8cm draft.

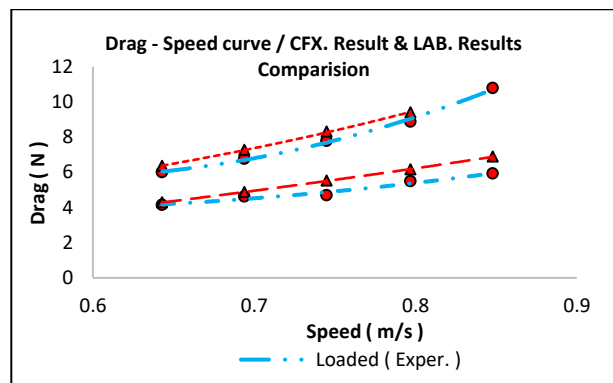


Figure 15. Comparison of the total resistance values of SALINA presented by the CFX and the experimental model

The results of a study conducted by Barrass (2004) addressing the very large crude carriers reveal that the ratio of frictional resistance to total resistance or drag is about 90%. Equation (4).

$$\frac{\text{Frictional Resistance}}{\text{Total Resistance}} = \% 90 \tag{4}$$

The results of calculating the frictional resistance and the total resistance of the SALINA model, which are obtained using the ITTC procedures and model tests performed in the towing tank, presented appropriate relationship between the total resistance and the frictional resistance. For example, the ratio of frictional resistance to the total resistance of the SALINA was about 83% in the draft of 16.5 meters (in the laden condition) and in the speed of 0.65m/s (ship speed of 12.5knots), The mentioned result is within the appropriate range as compared to the results of Barrass (2004).

$$\frac{R_F}{R_T} = \% 83 \quad (5)$$

In the present study, the mentioned ratio varies within the range of 83 to 91% for the Froude numbers of 0.13 to 0.16 (ship speeds of 12.5 to 16.5knots in calm water). To put in a nut shell, the mentioned finding is in line with the results of previous studies.

According to results of uncertainty analysis, carried out for the experimental model, at speeds of 0.65, 0.70, 0.75, 0.80 & 0.85m/s, the maximum uncertainty of the measured resistance in 8 and 16.5cm. drafts were found 0.89% & 0.77%, respectively.

#### 4. CONCLUSION

Approximately 90% of the resistance of all tankers is related to their frictional resistance and about 10% is related to their wave resistance. In ships in which the hull surface area outside the water is greater, such as passenger and container ships, frictional resistance is about 30 to 40%. Furthermore, wave resistance is one of the main factors affecting the variations in fuel consumption patterns of these ships. In this applied research, using a powerful computational fluid dynamics software (i.e., ANSYS CFX software) a numerical simulation of SALINA belonging to the National Iranian Tanker Company was presented. The mentioned model was used to calculate the drag force values of the ship's hull with consideration of the highest frequency of the actual service conditions over the last 4 years in the laden & ballast conditions (drafts of 8 and 16.5m) and at speeds of 12.5 to 16.5knots. In order to validate the obtained findings, the results of the numerical modeling were compared with the test results of the experimental model of SALINA performed in the towing tank. Based on the validations carried out, the difference between the results of the experimental and numerical models at low speeds was about 7% and at higher Froude numbers was observed to be up to 15%. Consideration of the difference in the calculated results presented in other studies, which varied from 5 to 17%, reveals that the computational error of the results obtained from this study is evaluated in an appropriate range.

#### 5. ACKNOWLEDGMENTS

The authors of the present article appreciate the valuable support of the technical & ship management director of the National Iranian Tanker Company, Mr. Akbar Jabal Ameli. Furthermore, a special gratitude is expressed to Dr. Hadi Mirzaei, Mr. Anooshirvan Yousefi Darestani, Dr. Shahriar Abtahi, and SALINA superintendent, Mr. Kambiz Moradi, who provided remarkable insights and contributions. Moreover, it is necessary to appreciate the detailed plans of the SALINA masters, including the late captain Majid Ghasabi Oruji and duty officers of the bridge and engine room of SALINA, who recorded and provided the key information needed during the voyage. We also sincerely appreciate Mr. Amir Mostashfi for his endless effort and effective and worthwhile support. His guidance increased the accuracy of the study and facilitated the implementation of the experimental tests of the model.

#### 6. REFERENCES

1. PARK, B J., SHIN, M-S., KI, M-S., LEE, G J., LEE, S B. *Experience in Applying ISO19030 to Field Data*. 2nd Hull Performance & Insight Conference. HullPIC'17. Ulrichshusen. 2017. March 27-29.p.150-155.
2. ZALEK, H. S. F., BECK, R. F., CECCIO, S. L. "High Speed Model Testing With Drag Reduction", University of Michigan, 2004.
3. VAN, S. H., KIM W. J., KIM, D. H., YIM, G. T., LEE, C. J., and EOM, J. Y., 1998. *Flow measurement around a 300K VLCC model*. Proceedings of the annual spring meeting, Ulsan, pp.185-188.
4. OGIWARA, S. and KAJITANI, H., 1994. *Pressure distribution on the hull surface of series 60 model*. Proceedings of CFD Workshop Tokyo, pp.350-358.
5. JONES, D. A., CLARKE, D. B., 2010. *Fluent code simulation of flow around a naval hull, the DTMB 5415*. Technical report, Defense Science and Technology Organization. DSTO-TR-2465, 30P.
6. OBREJA, D., POPESCUE, G, IONAS, O. and PACURARU, F., 2005. *Experimental techniques for vortices investigation around the ship model*, Workshop on Vortex Dominated Flows, Romania.
7. KORKUT and USTA., "Reduction of Ship Resistance through Induced Turbulent Boundary Layers", Master of Science in Ocean Engineering, Melbourne, Florida, 2010.
8. LUNGU, A., "Numerical Simulation of the Free-Surface Turbulent Flow around a VLCC Ship Hull", AIP Conference Proceedings 936, Corfu, Greece, 16-20 September 2007, p.647-650.

9. JAKOBSEN, K-R G., “*Turbulence modeling of transverse flow on ship hulls in shallow water*”, 2010.
10. HAKAN, O., BAYRAKTAR, S, and YILMAZ, T., 2007. *Computational investigation of a hull*, 2<sup>nd</sup> International Conference on Marine Research and Transportation, Italy, pp.145-150.
11. BANKS J, PHILLIPS AB, TURNOCK S. *Free surface CFD prediction of components of Ship Resistance for KCS*. 13th Numerical Towing Tank Symposium, Germany;2010.p. 1-7.
12. WHITE F. M., *Fluid Mechanics*, University of Rhode Island, 8<sup>th</sup> Edition, McGraw-Hill Education; 2015.p.864
13. NOBLESSE F., HUANG F. and YANG C. *The Neumann-Michell theory of ship waves*[J]. Journal of Engineering Mathematics, 2013, 79(1): 51-71.
14. HUANG F., YANG C. and NOBLESSE F. *Numerical implementation and validation of the Neumann-Michell theory of ship waves*[J]. European Journal of Mechanics-B/Fluids, 2013, 42: 47-68.
15. YANG C., NOBLESSE F., HUANG F., *Practical evaluation of the drag of a ship for design and optimization*, Journal of hydrodynamic, Volume 25, Issue 5, October 2013, Pages 645-654.
16. EBRAHIMI, A., *Numerical Study on Resistance of a Bulk Carrier Vessel Using CFD Method*, Journal of the Persian Gulf (Marine Science)/Vol. 3/No. 10/December 2012/6/1-6.
17. BARRASS B., *Ship design and performance for masters and mates*. 1<sup>st</sup> Edition. Butterworth-Heinemann; 2004.p.264.